Uplink Power Analysis of RIS-assisted Communication Over Shared Radar Spectrum

Mai Kafafy[a], Ahmed S. Ibrahim[b], Mahmoud H. Ismail[c,a]
[a]Electronics and Electrical Communications Engineering Dept., Cairo University, Giza, 12613, Egypt
[b]Electrical and Computer Engineering Dept., Florida International University, Miami, FL 33174, USA
[c]Electrical Engineering Dept., American University of Sharjah, PO Box 26666, Sharjah, UAE
mai.b.s.ali@eng.cu.edu.eg, aibrahim@fiu.edu, mhibrahim@aus.edu

***Abstract*—The wide deployment of wireless sensor networks has two limiting factors: the power-limited sensors and the congested radio frequency spectrum. A promising way to reduce the transmission power of sensors, and consequently prolonging their lifetime, is deploying reconfigurable intelligent surfaces (RISs) that passively beamform the sensors transmission to remote data centers. Furthermore, spectrum limitation can be overcome by spectrum sharing between sensors and radars. This paper utilizes tools from stochastic geometry to characterize the power reduction in sensors due to utilizing RISs in a shared spectrum with radars. We show that allowing RIS-assisted communication reduces the power consumption of the sensor nodes, and that the power reduction increases with the RISs density. Furthermore, we show that radars with narrow beamwidths allow more power saving for the sensor nodes in its vicinity.**

***Index Terms*—Reconfigurable intelligent surface, wireless communication, radars, spectrum sharing**

I. Introduction

Providing ubiquitous connectivity for Internet of Things (IoT) devices is challenging due to spectrum and power limitations. One way to overcome spectrum limitation is enabling communication over the radar spectrum [1]. For example, [2] proposed IoT connectivity in radar bands using zone-based spectrum sharing where IoT devices near the radar (i.e., inside its guard zone) are only allowed temporal access to the radar spectrum when the radar beam points elsewhere. Temporal radar spectrum sharing was also considered in [3] and [4], in which the downlink performance of communication systems in the vicinity of rotating radars was analyzed. This paper, too, assumes temporal spectrum sharing between Sensor Nodes (SNs) and a nearby radar; however and unlike the above works, it focuses on reducing the uplink transmission power of the SNs over the shared spectrum by deploying Reconfigurable Intelligent Surfaces (RISs) to assist communication between the SNs and their Fusion Centers (FCs).

RISs are surfaces that consist of a large number of reconfigurable reflecting elements. They are considered passive as they beamform the incident signals without transmitting any power of their own; this beamforming is attained by tuning the phases of the RIS reflecting elements through low power electronic circuits [5], [6]. Thus, RISs can reduce the required SN transmission power by beamforming its signal to the FC. The research body on RISs has been growing recently with different papers focusing on different RIS deployment scenarios [6]–[9]. For example, RIS phases were optimized to maximize different objectives of RIS-assisted communications in [10]–[15]. To elaborate, rate maximization in single and multi user Multi-Input-Single-Output (MISO) setups was considered in [10] and [11], respectively. Moreover, spectral efficiency maximization in MISO and Multi-Input-Multi-Output (MIMO) setups was considered in [12], [13]. Furthermore, SINR and energy efficiency were maximized in [14], [15]. However and to the best of our knowledge, this is the first work that considers using RIS-assisted uplink communication between SNs and remote FCs in a temporal spectrum sharing scenario with a nearby radar to reduce the SNs transmission power, which is vital due to the power limited nature of wireless SNs.

To elaborate more, in this paper, we use tools from stochastic geometry to analyze the SN transmission power required for successful RIS-assisted uplink communication between SNs and FCs over a shared radar spectrum. We derive the Cumulative Density Function (CDF) of the SN transmission power as a function of the RIS density and the radar parameters. Results show that enabling RIS-assisted communication reduces the required SNs transmission power, which is essential to prolong their lifetime. Moreover, we show how this power reduction is affected by different design and system parameters such as the RIS density and number of reflecting elements, as well as the direction and width of the radar beam.

The rest of this paper is organized as follows: the system model is described in Section II, the power CDF is derived in Section III, and the results are presented in Section IV before the paper is finally concluded in Section V.

II. System Model

Consider uplink communication between SNs and remote FCs that takes place on a shared radar spectrum. We consider, without loss of generality, a circular region of radius Z with the radar located at the center and the FCs on the perimeter. The FCs locations follow a Poisson Point Process (PPP) Φ_F with line density ζ_F (m^{-1}) such that the number of FCs on the circle perimeter is a Poisson random variable (RV) and their azimuth locations, denoted by θ_f^F, are independent and identically distributed (i.i.d.) uniform RVs over $[0, 2\pi]$ for all $f \in \Phi_F$. Let P_R denote the transmit power of the radar and Θ_R and Θ_{BW} be the direction and width of the radar beam, respectively.

RISs are used to improve communication by providing extra indirect paths between the SNs and the FCs. The RISs are randomly located inside the region and follow a PPP Φ_S with density ζ_S (m^{-2}). We consider the RISs to be electrically small and passive reflect array based with each RIS consisting of M reflecting elements (i.e., the RIS is considered a small-size scatterer with the size of each of its M reflecting element being around half the wavelength) [5], [7]. Element m of RIS s has reconfigurable reflection coefficient $\beta_{sm}e^{j\delta_{sm}}$ with $\delta_{sm} \in [0, 2\pi]$ being the phase and $\beta_{sm} \in [0, 1]$ the magnitude.

Due to the azimuth symmetry of the model, we focus our analysis on an SN located at $(x, 0)$. In order not to interfere with the radar operation, the SN transmits only when not in the radar beam. We denote the distance between two general points i and j in the network by $d_{ij} = \sqrt{r_i^2 + r_j^2 - 2r_i r_j \cos(\theta_i - \theta_j)}$, where $(r_i,\ \theta_i)$ are the polar coordinates of point i. The signal received from the SN at FC $f \in \Phi_F$ through RIS $s \in \Phi_S$ consists of two terms as follows [5]:

$$y_{xsf} = \sqrt{G}\left(\frac{h_{xf}}{d_{xf}^{\frac{\alpha}{2}}} + \sum_{m=1}^{M} \beta_{sm} e^{j\delta_{sm}} \frac{h_{xms}}{d_{xs}^{\frac{\alpha}{2}}} \frac{h_{smf}}{d_{sf}^{\frac{\alpha}{2}}}\right) t_x, \quad (1)$$

where t_x is the transmitted signal of the SN, G is the receive antenna power gain of the FC, and α is the path loss exponent. The first term in (1) is the signal received over the direct channel from the SN to FC f, denoted by h_{xf}. The second is the signal received over the indirect channel through the RIS with h_{xms} and h_{smf} denoting the channels from the SN to element m on RIS s and from element m on RIS s to FC f. Since the RISs are electrically small and reflect array based, the channels h_{xms} (and h_{smf}) can be considered independent for all reflecting elements m on the RIS. Moreover, the distances between the SN (or the FC) and the RIS can be considered the same for all reflecting elements on the RIS. For simplicity, we assume that all β_{sm} have the same binary value $\beta_s \in \{0, 1\}$ such that a typical RIS is in a reflecting mode (i.e., operating) when its $\beta = 1$ and silent otherwise.

To maximize the magnitude of the received signal, an FC f tunes the values of δ_{sm} to align the phases of the different components of y_{xsf} such that $\delta_m = \angle h_{xf} - \angle h_{xms} - \angle h_{smf}$, where $\angle\cdot$ denotes the phase. In this case, the average power of the received signal becomes

$$\begin{aligned}\mathbb{E}\left(|y_{xsf}|^2\right) &= pG.\mathbb{E}\left(\frac{|h_{xf}|}{d_{xf}^{\frac{\alpha}{2}}} + \sum_{m=1}^{M} \frac{|h_{xms}||h_{smf}|}{(d_{xs}d_{sf})^{\frac{\alpha}{2}}}\right)^2 \\ &\overset{a}{\approx} pG\left(d_{xf}^{-\alpha} + M^2(d_{xs}d_{sf})^{-\alpha}\right), \quad (2)\end{aligned}$$

where p is the SN transmission power and $\mathbb{E}(\cdot)$ is the expectation operator. The line $\overset{a}{\approx}$ is obtained by assuming independent channels with $\mathbb{E}(|h|^2) = 1$ and ignoring the cross multiplication terms. Clearly, tuning the RIS parameters requires knowledge of channel state information and exchanging control messages with local Radio Frequency (RF) controllers that reconfigure the RIS phases. Consequently and in order to reduce control overhead and undesired interference from RIS reflections, we assume that communication between the SN and the FC is assisted by a single RIS, which should be located outside the radar beam, while the rest of RISs are kept in silent mode (i.e., $\beta = 0$). Opposite to that, the radar is always active and consequently, it directly interferes with FCs whenever they lie in its beam.

Based on the above discussion, the signal-to-interference-plus-noise ratio (SINR) of the RIS-assisted communication from the SN to FC f through RIS s, denoted by γ_{xsf}, is [5], [16]

$$\gamma_{xsf} = \frac{\mathbb{E}\left(|y_{xsf}|^2\right)}{\sigma^2 + I} = \frac{pG}{\sigma^2 + I}\left(d_{xf}^{-\alpha} + M^2\left(d_{xs}.d_{sf}\right)^{-\alpha}\right), \quad (3)$$

where σ^2 and I denote the noise and radar interference powers at the FC, respectively. We assume a perfect radar radiation pattern such that the radar interference at FC $f \in \Phi_F$ is $I = P_R G Z^{-\alpha} 1\left(|\theta_f^F - \Theta_R| \le \Theta_{\text{BW}}\right)$ where θ_f^F is the azimuth location of FC f and the function $1(\cdot)$ is a binary indicator that equals 1 when its argument is true. Furthermore, we assume that an FC f successfully decodes the message of an SN at x when the SINR of the received message exceeds a threshold $\tilde{\gamma}$. Hence, the minimum required SN transmit power for successful decoding at FC f is given by

$$P_{\text{min},xf} = \frac{\tilde{\gamma}\left(\sigma^2 + I\right)/G}{d_{xf}^{-\alpha} + M^2 \max\limits_{s \in \Phi_{\text{out}}^S} \left(d_{xs}.d_{sf}\right)^{-\alpha}}, \quad (4)$$

where Φ_{out}^S is the set of RISs outside the radar beam (i.e., whose azimuth locations $\in [0, 2\pi] \setminus \left[\Theta_R - \frac{\Theta_{\text{BW}}}{2}, \Theta_R + \frac{\Theta_{\text{BW}}}{2}\right]$).

In the next section, we derive the CDF of the minimum SN transmission power required for successful decoding of its message.

III. Statistical Characterization of Uplink Transmission Power

The SN connects through the FC and the RIS that provide the lowest pathloss, and thus, requires the least transmit power. The minimum required transmission power of the SN at x is denoted by $P_{\text{min},x}$ and it takes the following form:

$$P_{\text{min},x} = \min_{f \in \Phi_F} P_{\text{min},xf}, \quad (5)$$

where $P_{\text{min},xf}$ is the minimum transmission power required for successful decoding at FC f as given in (4). Using order statistics [17], the CDF of $P_{\text{min},x}$ takes the following form

$$F_{P_{\text{min},x}}(p) = 1 - \mathbb{E}_{\Phi_{\text{in}}^F}\left(\prod_{f\in\Phi_{\text{in}}^F}\left(1 - F_{P_{\text{min},xf}}(p)\right)\right) \times$$
$$\mathbb{E}_{\Phi_{\text{out}}^F}\left(\prod_{f\in\Phi_{\text{out}}^F}\left(1 - F_{P_{\text{min},xf}}(p|I=0)\right)\right),$$
$$\overset{a}{=} 1 - \exp\left(-\zeta_F Z \int_{\theta_{\text{in}}} F_{P_{\text{min},xf}}(p) d\theta\right) \times$$
$$\exp\left(-\zeta_F Z \int_{\theta_{\text{out}}} F_{P_{\text{min},xf}}(p|I=0) d\theta\right). \quad (6)$$

The sets Φ_{in}^F and Φ_{out}^F include the FCs inside and outside the radar beam, respectively. The line $\overset{a}{=}$ is obtained using the probability generating functional (PGFL) of the PPP [18], where $\theta_{\text{in}} = \left[\Theta_R - \frac{\Theta_{\text{BW}}}{2}, \Theta_R + \frac{\Theta_{\text{BW}}}{2}\right]$ is the range of azimuth angles that lie inside the radar beam, and $\theta_{\text{out}} = [0, 2\pi] \setminus \theta_{\text{in}}$ is the range of azimuth angles that lie outside the radar beam. Moreover, $F_{P_{\text{min},xf}}(p)$ is the CDF of $P_{\text{min},xf}$, which takes the form

$$F_{P_{\text{min},xf}}(p) = 1 - \Pr\left(\min_{s\in\Phi_{\text{out}}^S}\left(d_{xs}d_{sf}\right) \geq \tilde{d}_f\right)$$
$$= 1 - \mathbb{E}_{\Phi_{\text{out}}^S}\left(\prod_{s\in\Phi_{\text{out}}^S} 1\left(d_{xs}d_{sf} \geq \tilde{d}_f\right)\right), \quad (7)$$

where $\tilde{d}_f = \left(\frac{M^2 pG}{\tilde{\gamma}(\sigma^2+I) - d_{xf}^{-\alpha} pG}\right)^{\frac{1}{\alpha}}$ and $\Pr(\cdot)$ indicates the probability of an event. Using the PGFL yields

$$F_{P_{\text{min},xf}}(p) = 1 - 1\left(d_{xf} \geq \frac{pG}{\tilde{\gamma}(\sigma^2+I)}\right) \exp\left(-\zeta_S \iint_{\mathcal{S}_f} r dr d\theta\right), \quad (8)$$

where $\mathcal{S}_f$ is the set of (r, θ) satisfying the conditions $r \in [0, Z]$, $\theta \in [0, 2\pi] \setminus \left[\Theta_R - \frac{\Theta_{\text{BW}}}{2}, \Theta_R + \frac{\Theta_{\text{BW}}}{2}\right]$, and $\tilde{d}_f \geq \sqrt{\left(Z^2 + r^2 - 2Zr\cos\left(\theta_f^F - \theta\right)\right)(x^2 + r^2 - 2xr\cos\theta)}$. Generally, $F_{P_{\text{min},xf}}(p)$, and hence $F_{P_{\text{min},x}}(p)$, do not have closed forms. Thus, we derive in Theorem 1 a closed form expression for the CDF of the worst case SN transmission power, which occurs when $\zeta_S \approx 0$. This worst case CDF serves as a lower bound to the exact CDF $F_{P_{\text{min},x}}(p)$.

Theorem 1. *In the case when $\zeta_S \approx 0$, $F_{P_{min,x}}(p)$ has the following closed form*

$$F_{P_{min,x}}(p) = 1 - \exp\left(-\zeta_F Z \mathcal{I}\right), \quad (9)$$

where

$$\mathcal{I} = 2\Theta^{out} + \sum_{i=1}^{2} 1\left(\omega_i^{in} \leq \Omega_i^{in}\right)\left(\Omega_i^{in} - \omega_i^{in}\right)$$
$$- \sum_{i=1}^{2} 1\left(\omega_i^{out} \leq \Omega_i^{out}\right)\left(\Omega_i^{out} - \omega_i^{out}\right). \quad (10)$$

The values of $\Omega^{out\,(in)}$ and $\omega^{out\,(in)}$ are

$$\Omega^{out\,(in)} = \begin{cases} \min\left(\Theta_R + \frac{\Theta_{BW}}{2}, 2\pi\right), & i = 1 \\ \min\left(\Theta_R + \frac{\Theta_{BW}}{2}, \Theta^{out\,(in)}\right), & i = 2 \end{cases} \quad (11)$$

$$\omega^{out\,(in)} = \begin{cases} \max\left(\Theta_R - \frac{\Theta_{BW}}{2}, 2\pi - \Theta^{out\,(in)}\right), & i = 1 \\ \max\left(\Theta_R - \frac{\Theta_{BW}}{2}, 0\right), & i = 2 \end{cases}, \quad (12)$$

where

$$\Theta^{in} = \left|\cos^{-1}\left(\frac{x^2 + Z^2 - (\tilde{\gamma}(\sigma^2+I)/(Gp))^{-2/\alpha}}{2xZ}\right)\right|, \quad (13)$$

and Θ^{out} is the same as Θ^{in} but with $I = 0$.

Proof. When $\zeta_S \approx 0$, we can assume that the SN signal received at FC f over the direct link dominates that received over the indirect link such that $\gamma_{xsf} \approx pGd_{xf}^{-\alpha}/(\sigma^2 + I)$ and

$$F_{P_{\text{min},xf}}(p) = 1\left(d_{xf} \leq \left(\frac{\tilde{\gamma}}{Gp}\left(\sigma^2 + I\right)\right)^{\frac{-1}{\alpha}}\right), \quad (14)$$

which can be written as

$$F_{P_{\text{min},xf}}(p) = 1\left(|\theta_f^F| \leq \Theta^{\text{out (in)}}\right) \forall f \in \Phi_{\text{out (in)}}^F, \quad (15)$$

and thus,

$$F_{P_{\text{min},xf}}(p) = 1 - \exp\left(-\zeta_F Z\left(\int_{\mathcal{F}_{\text{in}}} d\theta^F + \int_{\mathcal{F}_{\text{out}}} d\theta^F\right)\right), \quad (16)$$

where

$$\mathcal{F}_{\text{out}} = [0, 2\pi] \setminus \left[\Theta_R - \frac{\Theta_{\text{BW}}}{2}\right] \cap \left([2\pi - \Theta^{\text{out}}, 2\pi] \cup [0, \Theta^{\text{out}}]\right), \quad (17)$$

and

$$\mathcal{F}_{\text{in}} = \left[\Theta_R - \frac{\Theta_{\text{BW}}}{2}\right] \cap \left([2\pi - \Theta^{\text{in}}, 2\pi] \cup [0, \Theta^{\text{in}}]\right). \quad (18)$$

Knowing that $A \setminus B = A - A \cap B$, and that for two disjoint sets B and C, $A \cap (B \cup C) = A \cap B + A \cap C$, we can write $\mathcal{F}_{\text{out}}$ as $[2\pi - \Theta^{\text{out}}, 2\pi] - [\omega_1^{\text{out}}, \Omega_1^{\text{out}}] + [0, \Theta^{\text{out}}] - [\omega_2^{\text{out}}, \Omega_2^{\text{out}}]$ and $\mathcal{F}_{\text{in}}$ as $[\omega_1^{\text{in}}, \Omega_1^{\text{in}}] + [\omega_2^{\text{in}}, \Omega_2^{\text{in}}]$. □

IV. Numerical Results

This section presents the numerical results. All figures are generated from MATLAB Monte-Carlo simulations using the parameters in Table I, unless stated otherwise.

Figure 1 shows the effect of RIS deployment density, ζ_S, on the SN transmission power CDF. As seen, Theorem 1 well approximates the CDF at low ζ_S. The figure also shows that increasing ζ_S reduces the SN transmission power required for successful communication (i.e., shifts the CDF to the

TABLE I
SIMULATION PARAMETERS

Parameter	Value
Radius of region of interest, Z	2 km
Density of FCs, ζ_F	0.4 km^{-1}
SINR threshold, $\tilde{\gamma}$	5 dB
Path-loss exponent, α	2
Noise power, σ^2	-60 dBm
FC receive antenna gain, G	16 dB
Number of RIS reflecting elements, M	100
SN location, x	1 km
Density of RISs, ζ_S	0.8 km^{-2}
Radar wavelength, λ	0.0833 m
Radar transmission power, P_R	22 kW
Radar direction, Θ_R	90°
Radar beamwidth, Θ_{BW}	30°

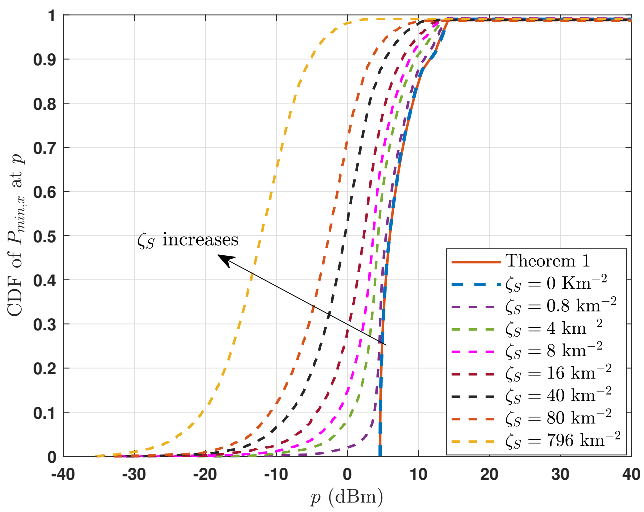

Fig. 1. Effect of RIS deployment density on the CDF of required SN transmission power.

left). This is because increasing ζ_S increases the number of available RISs, and consequently allows the SN to connect through the RIS and FC that provide the lowest pathloss.

Figure 2 shows that increasing the number of reflecting elements, M, per RIS reduces the required SN transmission power because it increases the number of parallel channels between the SN and FC, and consequently, improves the received signal strength. However it should be noticed that increasing M means bigger RISs and more phases to tune.

Next, Fig. 3 shows the CDF of the required transmission power of two SNs located at $x = 0.5$ km and 1 km. As seen, the SN near the zone perimeter (e.g., $x = 1$ km) generally requires less transmission power as it is closer to FCs, and therefore has lower path-loss. Increasing ζ_S generally reduces the required transmission power of the two SNs. Moreover, it reduces the gap between the power CDFs of the two SNs as the SN at $x = 0.5$ (which is far from FCs) benefits more from the SINR improvement of RIS-assisted communication.

Finally, Figs. 4 and 5 show the effect of the radar direction and beamwidth on the required SN transmission power CDF. As seen in Fig. 4, the SN needs less transmission power

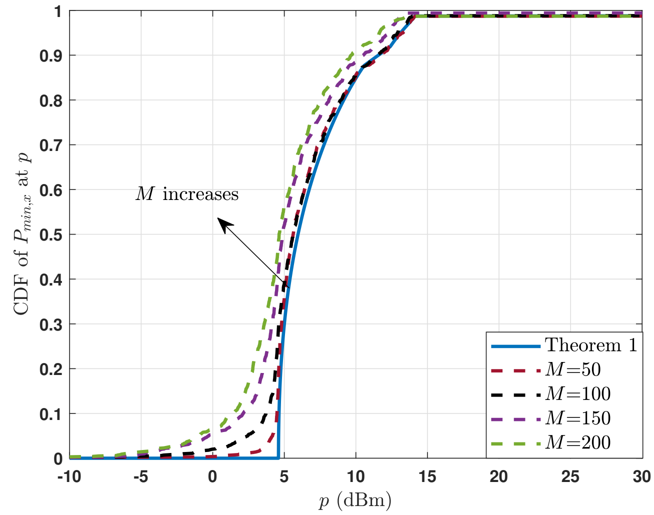

Fig. 2. Effect of the number of reflecting elements per RIS on the CDF of required SN transmission power.

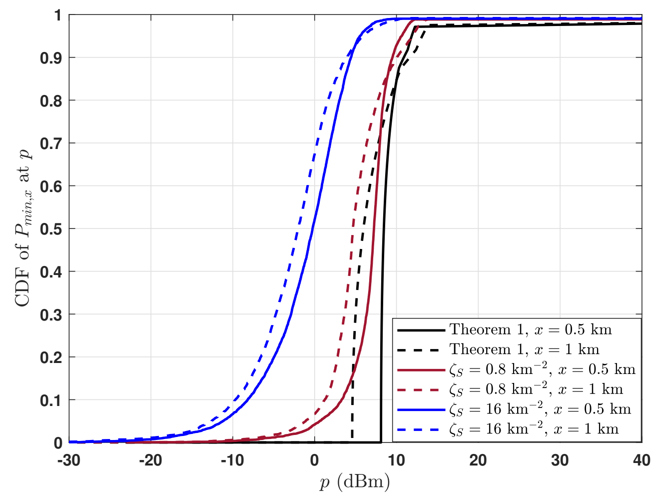

Fig. 3. CDF of required transmission power of SNs at different locations.

when the radar direction is opposite to the SN location (i.e., $\Theta_R = 180°$) because the radar does not interfere with the FCs near the SN as they are not in its beam. Moreover, the RISs near the SN are not silent for the same reason. Finally, as observed from Fig. 5, a wider radar beamwidth increases the required SN transmission power as the beam covers more FCs and RISs, and consequently, interferes with more FCs and silences more RISs. However, as seen from Fig. 5, increasing the RIS density reduces the effect of the radar beamwidth on the required transmission power as it offers the SN better connection links, in terms of path-loss, to the FC.

V. SUMMARY AND CONCLUSIONS

This paper shows that using RIS-assisted uplink communication between sensors and fusion centers in wireless sensor networks reduces the required transmission power of the sensors, and consequently prolongs their lifetime. The results

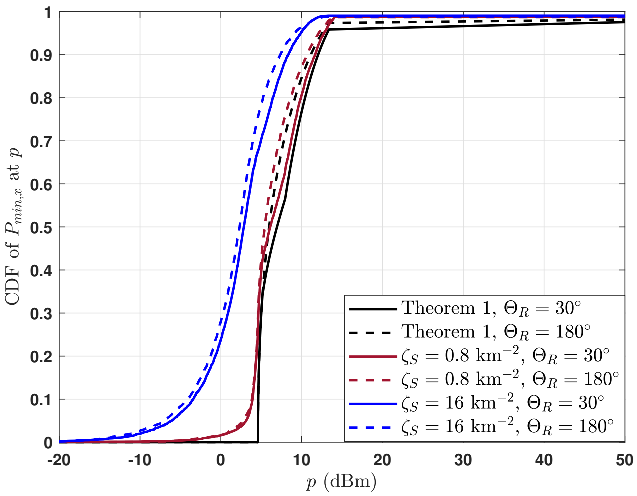

Fig. 4. Effect of radar direction on the CDF of required SN transmission power.

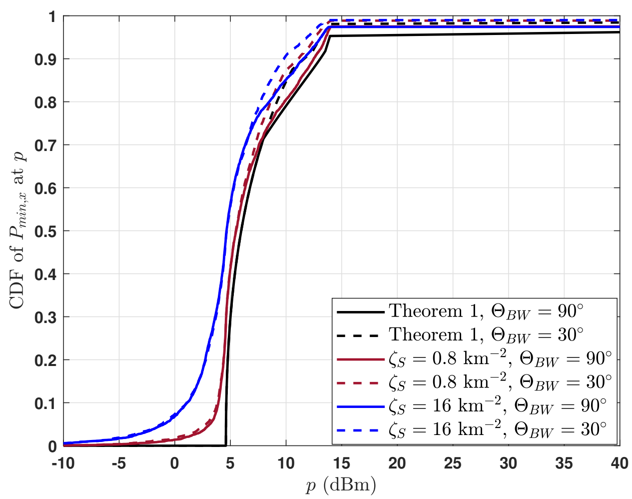

Fig. 5. Effect of radar beamwidth on the CDF of required SN transmission power.

show that the amount of reduction depends on many factors including the RIS density, the number of reflecting elements, and the parameters of the radar with which the spectrum is shared. The work in this paper can be extended to include the overhead of channel estimation and phase tuning of the RISs.

Acknowledgement

This work was supported by the American University of Sharjah under Grants no. EN0281:SCRI18-07 and FRG20-M-E10. The work of Ahmed S. Ibrahim was supported in part by the National Science Foundation under Award CNS-1816112.

References

[1] F. Liu, C. Masouros, A. P. Petropulu, H. Griffiths, and L. Hanzo, "Joint radar and communication design: Applications, state-of-the-art, and the road ahead," *IEEE Transactions on Communications*, vol. 68, no. 6, pp. 3834–3862, 2020.

[2] Z. Khan, J. J. Lehtomaki, S. I. Iellamo, R. Vuohtoniemi, E. Hossain, and Z. Han, "IoT connectivity in radar bands: A shared access model based on spectrum measurements," *IEEE Communications Magazine*, vol. 55, no. 2, pp. 88–96, 2017.

[3] F. Hessar and S. Roy, "Spectrum sharing between a surveillance radar and secondary Wi-Fi networks," *IEEE Transactions on Aerospace and Electronic Systems*, vol. 52, no. 3, pp. 1434–1448, 2016.

[4] M. Kafafy, A. S. Ibrahim, and M. H. Ismail, "Stochastic geometry-based performance analysis of cellular systems in the vicinity of rotating radars," *IEEE Communications Letters*, vol. 25, no. 4, pp. 1391–1395, 2021.

[5] M. A. ElMossallamy, H. Zhang, L. Song, K. G. Seddik, Z. Han, and G. Y. Li, "Reconfigurable intelligent surfaces for wireless communications: Principles, challenges, and opportunities," *IEEE Transactions on Cognitive Communications and Networking*, vol. 6, no. 3, pp. 990–1002, 2020.

[6] E. Basar, M. Di Renzo, J. De Rosny, M. Debbah, M.-S. Alouini, and R. Zhang, "Wireless communications through reconfigurable intelligent surfaces," *IEEE access*, vol. 7, pp. 116753–116773, 2019.

[7] Y. Liu, X. Liu, X. Mu, T. Hou, J. Xu, M. Di Renzo, and N. Al-Dhahir, "Reconfigurable intelligent surfaces: Principles and opportunities," *IEEE Communications Surveys Tutorials*, vol. 23, no. 3, pp. 1546–1577, 2021.

[8] M. Di Renzo, A. Zappone, M. Debbah, M.-S. Alouini, C. Yuen, J. De Rosny, and S. Tretyakov, "Smart radio environments empowered by reconfigurable intelligent surfaces: How it works, state of research, and the road ahead," *IEEE Journal on Selected Areas in Communications*, vol. 38, no. 11, pp. 2450–2525, 2020.

[9] S. Gong, X. Lu, D. T. Hoang, D. Niyato, L. Shu, D. I. Kim, and Y.-C. Liang, "Toward smart wireless communications via intelligent reflecting surfaces: A contemporary survey," *IEEE Communications Surveys & Tutorials*, vol. 22, no. 4, pp. 2283–2314, 2020.

[10] S. Abeywickrama, R. Zhang, Q. Wu, and C. Yuen, "Intelligent reflecting surface: Practical phase shift model and beamforming optimization," *IEEE Transactions on Communications*, vol. 68, no. 9, pp. 5849–5863, 2020.

[11] C. Huang, A. Zappone, M. Debbah, and C. Yuen, "Achievable rate maximization by passive intelligent mirrors," in *ICASSP*, pp. 3714–3718, 2018.

[12] X. Yu, D. Xu, and R. Schober, "MISO wireless communication systems via intelligent reflecting surfaces," in *ICCC*, pp. 735–740, 2019.

[13] B. Ning, Z. Chen, W. Chen, and J. Fang, "Beamforming optimization for intelligent reflecting surface assisted MIMO: A sum-path-gain maximization approach," *IEEE Wireless Communications Letters*, vol. 9, no. 7, pp. 1105–1109, 2020.

[14] S. M. Razavizadeh and T. Svensson, "3D beamforming in reconfigurable intelligent surfaces-assisted wireless communication networks," in *WSA*, pp. 1–5, 2020.

[15] Z. Yang, M. Chen, W. Saad, W. Xu, M. Shikh-Bahaei, H. V. Poor, and S. Cui, "Energy-efficient wireless communications with distributed reconfigurable intelligent surfaces," *IEEE Transactions on Wireless Communications*, 2021.

[16] E. Basar and H. V. Poor, "Present and future of reconfigurable intelligent surface-empowered communications [perspectives]," *IEEE Signal Processing Magazine*, vol. 38, no. 6, pp. 146–152, 2021.

[17] B. C. Arnold, N. Balakrishnan, and H. N. Nagaraja, *A first course in order statistics*. SIAM, 2008.

[18] J. G. Andrews, A. K. Gupta, and H. S. Dhillon, "A primer on cellular network analysis using stochastic geometry," *arXiv preprint arXiv:1604.03183*, 2016.